Control Trajectories for Interior Permanent Magnet Synchronous Motor Drives

M. E. Haque
School of Engineering
University of Tasmania
GPO Box 252-65 Hobart TAS 7001, Australia
E-mail: Enamul.Haque@utas.edu.au

M. F. Rahman
School of Electrical Engg & telecommunication
The University of New South Wales
Sydney NSW 2052, Australia
Email: f.rahman@unsw.edu.au

Abstract- **This paper presents an analysis of control trajectories for indirect and direct control of interior permanent magnet (IPM) synchronous motor drives. Since the inputs to the inner torque control loop of direct torque control (DTC) are the references for the torque and the amplitude of the stator flux linkage (λ_s), rather than $i_d.i_q$ plane in the indirect control, are transformed into the T-λ_s plane. The experimental results show the excellent performance of the indirect and direct torque controller, incorporating control trajectories.**

I. Introduction

Permanent magnet synchronous motors (PMSM) have become popular for high performance variable speed drive applications because of their high efficiency and compact construction. They offer the higher torque/volume compared to other motors by exploiting their rotor saliency. The IPM synchronous motor also offers the possibility of wider speed range, compared to their surface magnet version, due to the fact that the magnets are securely embedded inside the rotor iron. A substantially increased speed range can be obtained by flux weakening, thus allowing a constant power-like operation at speeds above the base speed level.

During the last decade, development has occurred in two main areas of permanent magnet (PM) motor drive. Firstly, various PM motor configurations of suitable values of the stator d- and q-axes inductances (L_d, L_q and L_q/L_d ratio) and method of reducing cogging torque. Secondly, various control strategies for the maximum torque per ampere (MTPA) characteristic and maximum flux weakening range have been studied [1-7]. All of this research used indirect torque and flux control strategies in which these two quantities were regulated by current controllers in the rotor dq-reference frame. A shaft encoder associated coordinate transformation and current control networks are mandatory in these schemes. The delays suffered through these networks by the control signals are known to be responsible for similar delay in the torque responses.

With the appearance of high-speed digital signal processors (DSP's), a control method called direct torque control (DTC) has become popular both in induction and permanent magnet synchronous motor (PMSM) drives [8-10]. Direct torque controlled IPM synchronous motor drive is a potential candiate in high performance and wide speed applications such as in electric vehicle. However, much attention has not yet been paid to the trajectory control of DTC. A good number of papers on the trajectory control of PMSM under PWM (pulse width modulation) current control in the constant torque [maximum torque per ampere (MTPA) trajectory] and the field-weakening (FW) region have been reported in literature [1-7]. Direct torque control with field weakening was reported in [11,12]. However, these work emphasized on high speed region and the complete trajectory control from zero speed to field weakening region has not been investigated.

In this paper, a complete trajectory control (constant torque operation and field wekening operation) from zero speed to field weakening region under DTC, using a Kolmorgan industrial IPM motor has been presented. The analyses of control trajectories are discussed in detail. The MTPA trajectory, current and voltage constraints are expressed in the T-λ_s plane. These have been incorporated into the DTC scheme. The experimental results show the excellent performance of the trajectory controller within the DTC.

II. Control Trajectories for Indirect Control of IPM Synchronous Motor Drive

The maximum torque capability of IPM synchronous motor is limited by the voltage and current ratings of the machine as well as those of the inverter. Therefore, under these two conditions, it is desirable to use a control scheme, which can yield the maximum torque per ampere over the entire speed range including the flux weakening operation. The d-axis component of the stator current is tightly regulated to zero in the conventional control method, and therefore the reluctance torque is not utilized even if the motor has some saliency. For high torque and high efficiency operations of IPM synchronous motors, it has been demonstrated that not only the q-axis current but also the d-axis current have to be controlled to satisfy the maximum torque-per-ampere trajectory for constant torque operation.

The torque for IPM synchronous motor in terms of stator flux linkage is given by;

$$T=\frac{3}{2}P\left(\lambda_d i_d-\lambda_q i_q\right)=\frac{3}{2}P[\lambda_f i_q+(L_d-L_q)i_d i_q] \quad (1)$$

In the d-q coordinate which rotate synchronously with an angular velocity, ω, the voltage equation can be expressed as follows;

$$\begin{bmatrix} v_d \\ v_q \end{bmatrix}=\begin{bmatrix} r+pL_d & -\omega L_q \\ \omega L_d & r+pL_q \end{bmatrix}\begin{bmatrix} i_d \\ i_q \end{bmatrix}+\begin{bmatrix} 0 \\ \omega\lambda_f \end{bmatrix} \quad (2)$$

The steady-state phasor diagram of an IPM synchronous motor is shown in figure 1, where β and γ are the leading angles of the stator current and voltage vectors from the q-axis respectively. The torque in terms of the amplitude of the stator current is as follows:

$$T = \frac{3}{2} P \lambda_f I_s \cos\beta + \frac{3}{4} P (L_q - L_d) I_s^2 \sin 2\beta \tag{3}$$

The first term of (3) is the excitation torque T_e and the second term is the reluctance torque T_r.

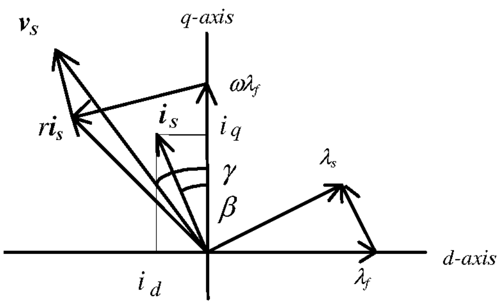

Figure 1. Phasor diagram of an IPM synchronous motor.

A. Maximum torque-per-ampere (MTPA) trajectory

As the IPM motor has a saliency ($L_d<L_q$) and the reluctance torque T_r is available, the armature current vector is controlled in order to produce the maximum torque-per-ampere. The relationship between i_d and i_q for the MTPA can be derived as [3]:

$$i_d = \frac{\lambda_f - \sqrt{\lambda_f^2 + 4(L_q - L_d)^2 i_q^2}}{2(L_q - L_d)} = \frac{\lambda_f}{2(L_q - L_d)} - \sqrt{\frac{\lambda_f^2}{4(L_q - L_d)^2} + i_q^2} \tag{4}$$

Equation (4) implies that the maximum torque-per-ampere (MTPA) is obtained if i_d is determined by (4) for any i_q. i_q could be determined by the outer control loops such as the speed loop, as is done in the existing literature. It should be noted here that the torque is not directly proportional to i_q. This is why the torque control via current control is called indirect torque control.

B. Current and voltage limit trajectories

Considering the voltage and current constraints, the armature current and voltage are limited by the constraints as follows:

$$I_s = \sqrt{i_d^2 + i_q^2} \le I_{sm} \tag{5}$$

$$V_s = \sqrt{v_d^2 + v_q^2} \le V_{sm} \tag{6}$$

where I_{sm} and V_{sm} are the available maximum current and voltage of the inverter/motor.

The analysis of the voltage constraint is based on the steady-state voltage equations for simplicity. Substituting (2) into (6) in the steady-state, yields

$$V_s = \sqrt{(ri_d - \omega L_q i_q)^2 + (ri_q + \omega L_d i_d + \omega\lambda_f)^2} \le V_{sm} \tag{7}$$

If the stator resistance is neglected, equation (7) can be simplified as,

$$(L_q i_q)^2 + (L_d i_d + \lambda_f)^2 \le (\frac{V_{sm}}{\omega})^2 \tag{8}$$

$$i_d = -\frac{\lambda_f}{L_d} + \frac{1}{L_d}\sqrt{\frac{V_{sm}^2}{\omega^2} - (L_q i_q)^2} = -\frac{\lambda_f}{L_d} + \frac{1}{L_d}\sqrt{i_{d1}} \tag{9}$$

where, $i_{d1} = \frac{V_{sm}^2}{\omega^2} - (L_q i_q)^2$

C. Voltage limited maximum output trajectory

The armature current vector $i_3(i_{d3}, i_{q3})$ producing maximum output power under the voltage limit condition is derived as follow [13]

$$i_d = -\frac{\lambda_f}{L_d} - \Delta i_d \quad (9) \qquad i_q = \frac{\sqrt{\left(\frac{V_{sm}}{\omega}\right)^2 - (L_d \Delta i_d)}}{\rho L_d} \tag{10}$$

$$\Delta i_d = \frac{-\rho\lambda_f + \sqrt{(\rho\lambda_f)^2 + 8(\rho - 1)^2 \left(\frac{V_{sm}}{\omega}\right)^2}}{4(\rho - 1)L_d} \tag{11}$$

where, $\rho = \frac{L_q}{L_d}$

The current vector trajectory of the voltage limited maximum output is shown in figure 2(b). The rotor speed ω_p is the minimum speed for the voltage-limited maximum-output operation. Below this speed, the voltage-limited maximum-output operating point can not be reached, because the voltage-limited maximum-output trajectory intersects the voltage limit trajectory outside the current limit circle. If $\lambda_f / L_d > I_{sm}$, the voltage-limited maximum output trajectory is outside the current-limit trajectory. Therefore, voltage-limited maximum-output trajectory needs not to be considered

The control trajectories satisfying the MTPA characteristic and current and voltage limit constraints are drawn for the motor in Table I in figure 2(b). The control modes, i.e., maximum torque-per-ampere and flux weakening controls, are selected according to the analysis of figure 2(b). The q-axis commanded current i_q^* is determined by the outer control loop and the d-axis commanded current i_d^* is decided by equations (4) in maximum torque-per-ampere control mode, or by (8) in flux weakening control mode. Whether MTPA mode or the field weakening mode should be selected is determined by the rotor speed and the load. According to the rotor speed, the motor operation is divided into three sections, that is, below the base speed ω_b, above the crossover speed ω_c and between the base and crossover speeds. The crossover speed ω_c is the speed at which the back emf voltage of the unloaded motor equals to the maximum voltage.

Figure 2 shows the block diagram and control trajectories in $i_d - i_q$ plane for indirect PWM current control (vector control). Figure 3 and 4 show experimental results under constatnt torque operation and field weakening operation.

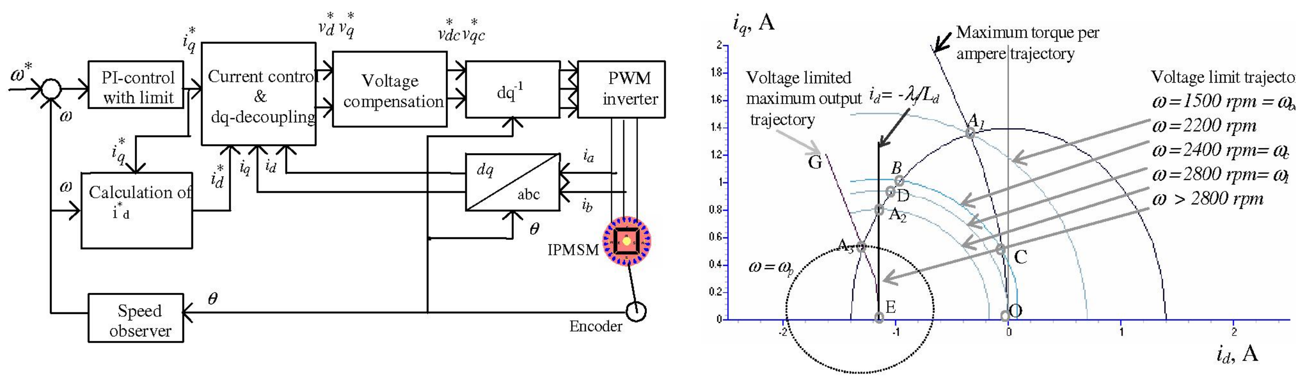

(a) Block diagram for PWM current control

(b) Control trajectories in the $i_d - i_q$ plane

Figure 2. Indirect PWM current control incorporating control trajectories in $i_d - i_q$ plane.

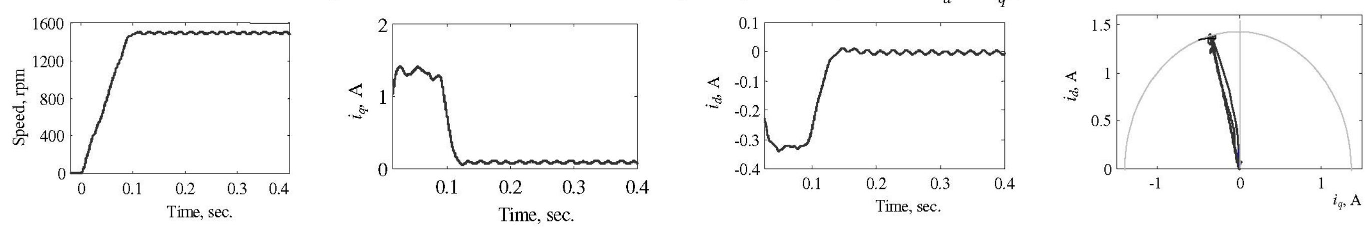

(a) speed response.

(b) i_q response.

(c) i_d response.

(d) Locus of current vector.

Figure 3. Dynamic response of indirect PWM current control, incorporating control trajectory under constant torque operation ($\omega_r \leq \omega_b$); Experimental results.

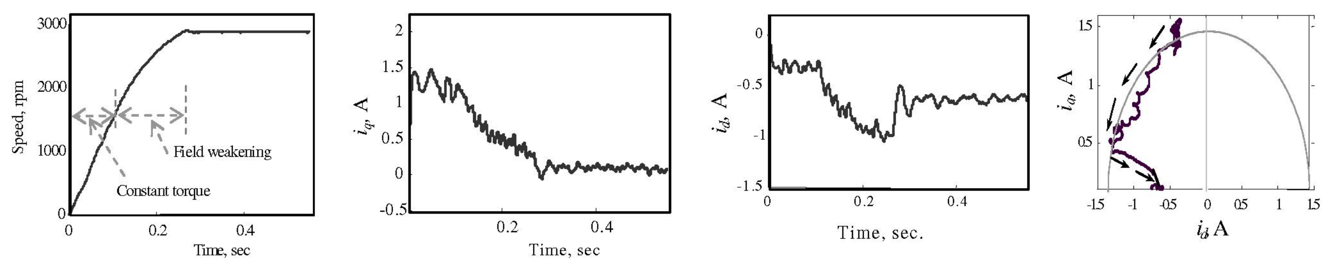

(c) speed response.

(d) i_q response.

(e) i_d response.

(f) Locus of current vector.

Figure 4. Dynamic response of indirect PWM current control, incorporating control trajectory under field weakening ($\omega_r > \omega_c$); Experimental results.

III. Control Trajectories for Direct Control of IPM Synchronous Motor Drive

Trajectory control techniques are employed to produce the torque or current references to achieve different goals in constant torque and field weakening ranges of operation. The control of the stator flux linkage should be based on the torque, and according to the control trajectories (MTPA, and field weakening trajectories) as shown in figure 2(b). These control trajectories in $i_d - i_q$ plane can also be adopted in the DTC of the IPM synchronous motor drives as is shown in later sections. Since the inputs to the inner torque control loop are the references for the torque and the amplitude of the stator flux linkage, rather than i_d and i_q, the control trajectories in $i_d - i_q$ plane are transformed into the torque and λ_s plane. Based on these trajectories in the new plane, λ_s is determined from the torque, which is the output of the speed controller, for constant torque and field weakening operations.

A. Maximum torque-per-ampere trajectory in torque-λ_s plane

The motor developed torque, in terms of the stator and rotor flux linkage amplitudes is also given by

$$T(k) = \frac{3p\hat{\boldsymbol{\lambda}}_{s(k)}}{4L_dL_q}\left[2\boldsymbol{\lambda}_f L_q \sin\{\delta(\kappa)\} - \hat{\boldsymbol{\lambda}}_{s(k)}(L_q - L_d)\sin 2\{\delta(\kappa)\}\right] \quad (12)$$

The stator flux linkage and δ are given by

$$\begin{cases} |\lambda_s| = \sqrt{\lambda_d^2 + \lambda_q^2} = \sqrt{(L_d i_d + \lambda_f)^2 + (L_q i_q)^2} \\ \delta = \left(\dfrac{L_q i_q}{L_d i_d + \lambda_f}\right) \end{cases} \quad (13)$$

As the IPM motor has a saliency ($L_q > L_d$) and the reluctance torque T_r is available, the armature current vector is controlled in order to produce the maximum torque-per-ampere. The relationship between i_d and i_q for the MTPA can be derived as [2]:

$$i_d = \frac{\lambda_f}{2(L_q - L_d)} - \sqrt{\frac{\lambda_f^2}{4(L_q - L_d)^2} + i_q^2} \tag{14}$$

If i_d and i_q are controlled according to the maximum torque-per-ampere trajectory as shown in equation (14), equation (13) is then rewritten as:

$$\begin{cases} \lambda_s = \sqrt{\lambda_f^2 - \left(\dfrac{L_d^2}{L_q - L_d} + L_q - L_d\right)\lambda_f i_d + (L_d^2 + L_q^2) i_d^2} \\ \delta = \tan^{-1}\left(\dfrac{L_q}{\lambda_f + L_d i_d}\sqrt{i_d^2 - \dfrac{\lambda_f}{L_q - L_d} i_d}\right) \end{cases} \tag{15}$$

It is possible to solve i_d from (14) and substitute it together with (13) into equation (1) to obtain the expressions for λ_s and δ in terms of torque. These expressions will be very complicated and difficult to solve in real time. The relationships among λ_s, δ and positive torque for the IPM motor can be found from the off-line calculation as shown in figure 4 for the IPM motor in Table II. For negative torque, δ becomes negative and λ_s remains the same. It is seen from figure 5 that both the amplitude λ_s and angle δ increase with the increase of torque. When the torque is zero, the angle is zero and the stator flux is equal to the magnet flux, which agrees with the analysis in the previous sections. As is also seen from this figure that the load angle δ is always below δ_m with the MTPA control when the torque is limited below the maximum torque the motor can produce. According to the torque equation (12), if two of the three variables, namely T, λ_s and δ, are known, the third one is uniquely determined. Provided the torque is known MTPA control is achieved if the amplitude or the angle of the stator flux is determined from the above figure, which can be stored in a look-up table. For the DTC, it is obvious that the amplitude of the stator flux rather than its angle should be controlled. When the torque and λ_s are controlled in this way, the angle δ will be automatically controlled and δ_m will not be exceeded. This is the requirement for the application of DTC in IPM synchronous motor drives.

B. Current and Voltage Constraints in Torque-λ_s Plane

The current and voltage constraints can be written as;

$$|i_d| = \sqrt{I_{sm}^2 - i_q^2} \quad (16) \qquad |v_d| = \sqrt{V_{sm}^2 - v_q^2} \quad (16)$$

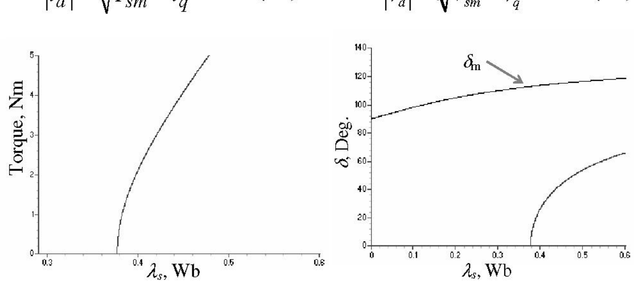

(a) Torque vs λ_s. (b) δ vs λ_s.

Figure 5 Torque and δ as a function of the amplitude of stator flux linkage for the maximum torque-per-ampere trajectory.

The current constraint is plotted in the torque-λ_s plane and δ-λ_s plane as shown in figure 6 for the IPM motor of Table II. It is seen from figure 6(b) that current limit trajectory is always below δ_m. If the stator resistance is neglected, the stator voltage is given by,

$$V_s = \omega_s \lambda_s \tag{17}$$

(7)

where ω_s is the rotational speed of the stator flux linkage. In the steady state, the rotational speeds of the stator flux linkage and the rotor magnet flux linkage are the same and equation (17) can be rewritten as:

$$V_s = \omega_r \lambda_s = \omega_b \lambda_{sr} = \omega_c \lambda_f \tag{18}$$

where ω_r, ω_b and ω_c are the rotor speed, base speed and crossover speed respectively. λ_{sr} is the rated stator flux linkage. ω_c is here defined to be the speed for which the unloaded motor develops the rated phase voltage V_{sm}. Maximum voltage trajectories for a motor can be determined by each (i_d, i_q) pair and a given speed, using Kirchhoff's voltage equation. For simplicity, the maximum voltage limit for each speed is indicated as a vertical line, as defined by equation (18).

The current limit and the MTPA trajectories for the IPM motor of Table II are superimposed in figure 6. The current limit is satisfied if the torque and λ_s are controlled below current limit trajectory. The intersection of the current limit and maximum torque-per-ampere trajectories is point *A*, which corresponds to the operating point with the maximum torque and current. If the torque is limited below the value at the operating point *A* for the MTPA control, the current limit is always satisfied. For constant torque operation, the amplitude of the stator flux is independent of the speed and is only dependent on the torque. While for field weakening operation, it is independent on the torque and is determined only by the rotor speed.

C. Control mode selection for constant torque and field weakening operations

For operation below the base speed, constant torque control should be selected. For the operation above the crossover speed, field-weakening control is undoubtedly selected since the voltage limit will no longer be satisfied if the torque and λ_s are controlled along the maximum torque-per-ampere trajectory. However, for the operation between the base speed and crossover speed, the torque determines the control mode. With the MTPA control, for instance, if the vertical dashed line in figure 6 represents the voltage limit corresponding to the operation with the rotor speed between ω_b and ω_c, there is an intersection of this line and the maximum torque-per-ampere trajectory, and at this point the torque is T_B. If the actual torque is greater than T_B, field-weakening control is selected. Otherwise, if the actual torque is smaller than T_B, constant torque control is selected even though the rotor speed is above the base speed. Figure 7 shows the flow chart for the control mode selection.

D. Implementation of the Trajectory Control for DTC

Figure 8 shows the complete block diagram of trajectory control under DTC. The look-up table is used to determine the amplitude of the stator flux linkage, according to the MTPA trajectory for constant torque control. The amplitude of the stator flux linkage is determined by the inverse of the speed for field weakening operation.

The DTC drive under trajectory control was implemented with the IPM synchronous motor of Table II. A digital signal processor TMS320C31 was used to carry out the DTC and trajectory control algorithms. The sampling time is 100 μs for inner torque and flux control loops and 500 μs for speed control loop.

Figure 9 shows experimental results under constatnt torque operation. Figure 9(a) and 9(b) show the speed and torque responses respectively, for a step change in speed reference from 0 to 1260 rpm. The maximum torque of the IPM motor under maximum torque-per-ampere control is 3.7 Nm. Figure 9(c) and 9(d) shows the stator flux locus and $T-\lambda_s$ trajectory, respectively.

Figure 10 shows the dynamic responses of the drive system with respect to a step change in speed reference from 0 to 1700 rpm. Figure 10(b) and (c) show the actual torque and λ_s waveforms. Figure 10(d) shows the locus of the stator flux linkage vector, which is a circle in both constant torque and field weakening operations. Figure 10(d) shows the torque and stator flux in the torque-λ_s plane for field weakening operation

The experimental results demonstrate that the drive is capable of working from zero speed to field weakening region and shows very good dynamic and steady state performance. . It is seen the transition between the constant torque and field weakening operations are very smooth

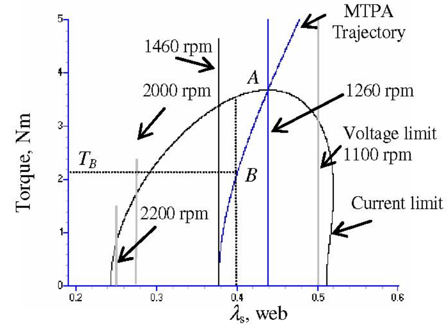

(a) Torque vs λ_s.

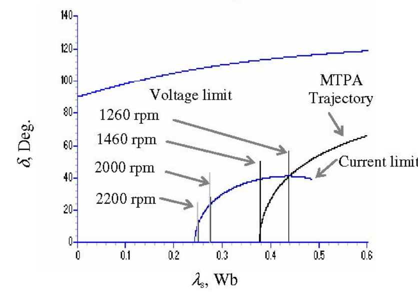

(b) δ vs λ_s.

Figure 6. Control trajectories in torque-λ_s plane

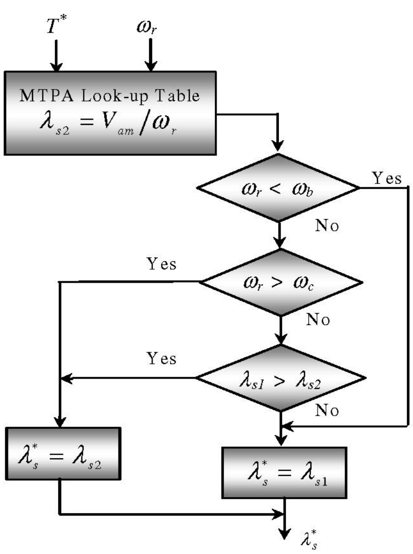

Figure 7. Flow chart for the control mode selection.

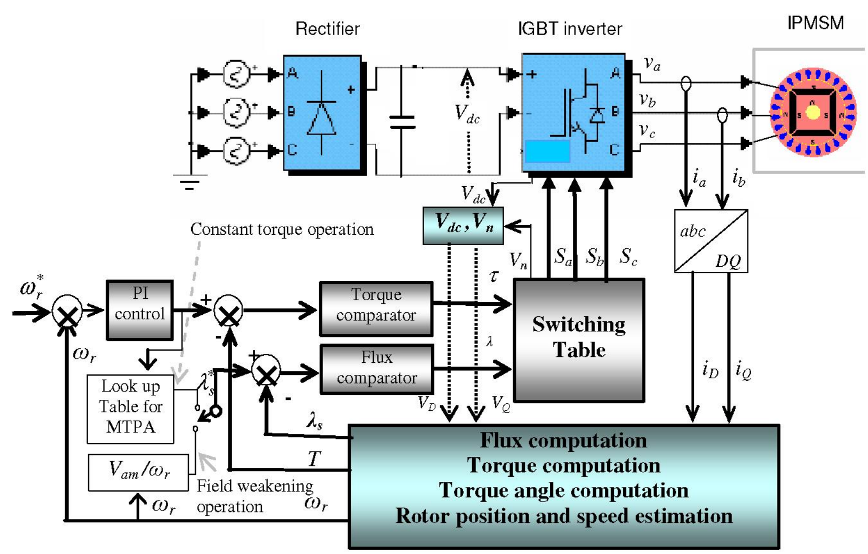

Figure 8. Direct torque control of IPM motor drive, incorporating control tracjectoriqes in T-λ_s Plane.

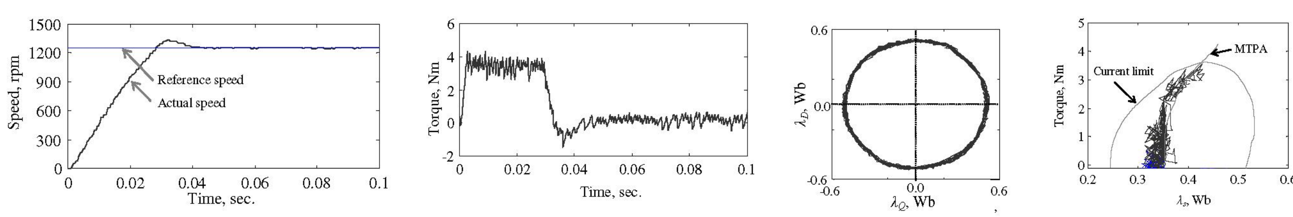

(a) Speed response

(b) Torque response

(c) Locus of the stator flux

(d) Torque versus λ_s

Figure 9. Dynamic responses of the DTC drive, incorporating control trajectories un der constant torque operation; Experimental results

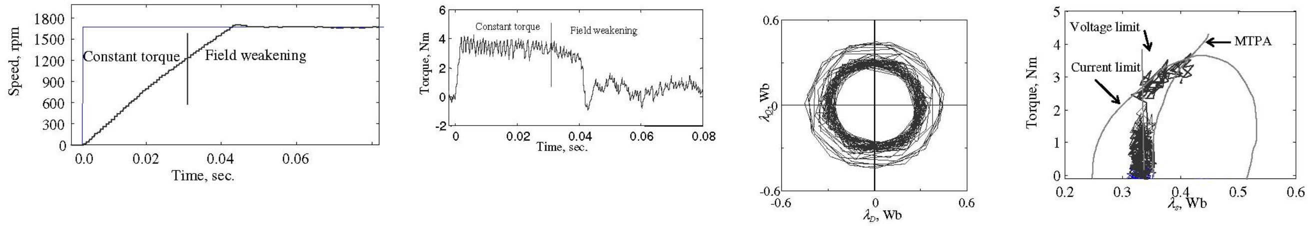

(a) Speed response (b) Torque response (c) Locus of the stator flux (d) Torque versus λ_s

Figure 10. Dynamic responses of the DTC drive, incorporating control trajectories; experimental results (constatnt torque and field weakening operation)

IV CONCLUSIONS

The analysis of control trajectories for indirect and direct controlof IPM synchronous mtoor drives has been presented in this paper. Then the experimental results for indirect and direct torque control incorporating control trajectories both in constant torque and field weakening operation has been provided. The maximum-torque–per-ampere trajectory, current and voltage constraints are expressed in the T-λ_s plane. These have been incorporated into the DTC scheme. The experimental results show the excellent performance of direct torque controller, incorporating control trajectories from zero speed to field weakening range**.** It is seen that the transition between the constant torque and field weakening operations are very smooth and the drive is capable of working from zero speed to field weakening region and shows very good dynamic and steady state performance

TABLE I
Prototype IPM synchronous motor parameters

Number of pole pairs, P	2
Stator resistance R	18.6 Ω
Magnet flux linkage λ_f	0.447 Wb
d-axis and q-axis inductance (L_d, L_q)	0.3885 H and 0.4755 H
Phase voltage and current (V and I)	240 V and 1.4 A
Base speed ω_b	1500 rpm
Crossover speed ω_c	2400 rpm
Rated torque T_b	1.95 Nm

Table II
Kolmorgan IPM synchronous motor parameters

Number of pole pairs, P	2
Stator resistance R	5.8 Ω
Magnet flux linkage λ_f	0.377 Wb
d-axis and q-axis inductance (L_d, L_q)	0.0448 H and 0.1024 H
Phase voltage and current (V and I)	132 V and 3 A
Base speed ω_b	1260 rpm
Crossover speed ω_c	1460 rpm
Rated torque T_b	3.7 Nm

REFERENCES

[1] T. M. Jahns, "Flux-weakening regime operation of an interior permanent magnet synchronous motor drive", *IEEE Trans. on Industry Applications,* vol. 23, pp. 398-407, 1987.

[2] S. Morimoto, M. Sanada, Y. Takeda, "Wide-speed operation of interior permanent magnet synchronous motors with high-performance current regulator", *IEEE Trans. on Industry Applications,* vol. 30, pp. 920-926, 1994.

[3] M. E. Haque, L. Zhong and M. F. Rahman, "Improved trajectory control for an interior permanent magnet synchronous motor drive with extended operating limit", *Journal of Electrical and Electronic Engineering, Institute of Engineers, Australia*, vol 22, no. 1, pp. 49-57, 2002.

[4] C. Pan and S. Sue, "A linear maximum torque per ampere control for IPMSM drives over full-speed range", IEEE *Transactions on Energy Conversion*, vol. 20, no. 2pp 359-366, June, 2005.

[5] B. Sneyers, D. W. Novotny, and T. A. Lipo, "Field weakening in buried permanent magnet ac drives," *IEEE Trans. Ind. Applicat.*, vol. IA-21, pp. 398–407, Mar./Apr. 1985.

[6] J. M. Kim and S. K. Sul, "Speed control of interior permanent magnetsynchronous motor drive for the flux-weakening operation," *IEEE Trans.Ind. Applicat.*, vol. 33, pp. 43–48, Jan./Feb. 1997.

[7] M. N. Uddin, T. S. Radwan, and M. A. Rahman, "Performance of interior permanent magnet motor drive over wide speed range," *IEEE Trans.Energy Convers.*, vol. 17, no. 1, pp. 79–84, Mar. 2002.

[8] I. Takahashi and T. Noguchi, "A new quick torque response and high efficiency control strategy of an induction motor", *IEEE IAS Annual Meeting,* pp. 496-502, 1985.

[9] M. F. Rahman, L. Zhong, W. Y. Hu, K. W. Lim and M. A. Rahman, "A direct torque controller for PM synchronous motor drives", *IEEE Trans. on Energy Conversion*, pp. 637-642, Sept. 1997.

[10] M. E. Haque, L. Zhong and M. F. Rahman, "A sensorless initial rotor position estimation scheme for a direct torque controlled interior permanent magnet synchronous motor drive", *IEEE Transaction on Power Electronics* vol. 18, no. 6, pp. 1376-1383, Nov. 2003.

[11] M. F. Rahman, L. Zhong, W. Y. Hu, K. W. Lim and M. A. Rahman, **"**A direct torque controlled interior permanent magnet synchronous motor drive incorporating field weakening**",** *IEEE Transaction onIndustrial applications*, vol.. 34, no. 6, pp. 1246-1253, Dec. 1998.

[12] M. Zordan, P. Vas, M. Rashed, S. Bolognani, M. Zigliotto, "Field-weakening in high-performance PMSM drives: a comparative analysis", IEEE Industry Application conference, vol. 3, pp. 1718-1724, Oct. 8-12, 2000.

[13] S. Morimoto, M. Sanada, Y. Takeda, "Expansion of operating limits for permanent magnet motor by current vector control considering inverter capacity", *IEEE Trans. on Industry Applications,* vol. 26, pp. 866-871, 1990.